Ajibola A. Bayode[1,*]
Hamza Badamasi[2]
Johnson Adedeji Olusola[3,4]
Solomon S. Durodola[5]
Olaniran K. Akeremale[6]
Odunayo T. Ore[5]
Brigitte Helmreich[7]
Martins O. Omorogie[1,7,8,*]

One-Pot Synthesis of ZnO-Activated Eggshell@kaolinite: Sorbents for Phosphate Capture in Water

The availability of colossal amounts of phosphate in water bodies has led to serious environmental challenges all over the world. In this study, a new adsorbent was synthesized using treated kaolinite clay, pulverized eggshells, and $ZnCl_2$. Surface characterizationof these adsorbents showed the availability of functional moieties, morphological variations, pore sizes, particle sizes, etc. Adsorption of phosphate occurs via multiple mechanisms, comprising ligand exchange, complexation, hydrogen bonding, and electrostatic interaction, among others. The effect of pH, showed that maximum adsorption of 93.3 % was achieved at pH 3.0. It was also shown that these cost-effective adsorbents could be regenerated in six cycles, hence increasing their applicability.

Keywords: Adsorption, Calcite, Eggshell, Phosphate, Sustainable materials

Received: March 29, 2023; *revised:* August 28, 2023; *accepted:* October 19, 2023

DOI: 10.1002/ceat.202300176

Supporting Information available online

1 Introduction

Phosphorus is an essential nutrient for plants, animals, and humans. Under natural conditions, it is typically scarce in water; however, human activities have resulted in excessive loading of phosphorus into surface waters, which can cause water pollution by promoting excessive algae growth, eutrophication particularly in lakes and rivers [1–3], and environmental degradation. Therefore, phosphorus is on the list of substances in the European Union that have to be considered to achieve a "good surface water chemical status" and which contribute to eutrophication [4].

In addition, the reduction or the total removal of phosphate from water is a necessity for both drinking water purposes and wastewater treatment, to prevent the many harmful risks such as kidney damage, hepatocellular carcinoma, and osteoporosis linked to excessive phosphate ingestion [5–8].

Different technologies have been explored for the sequestration of dissolved phosphate from water, which include advanced biological treatment, chemical precipitation, ion exchange, electrodialysis, membrane filtration, electro-coagulation, and adsorption [9–21]. The major shortcomings of some of these techniques include the operational cost, difficulties in operation, and limited versatility. Apart from chemical precipitation, which is the main removal technique in sewage treatment plants, the adsorption technique has been favored over other techniques because it is cost-effective and efficient and can also be used to solve the problem of nutrient recovery [5, 17, 19, 22, 23].

However, successful optimal removal using the adsorption technique depends on the choice of adsorbent. As traditional methods of phosphate removal continue to be explored, unconventional and sustainable alternatives are also gaining massive attention [24]. Over the years, different adsorbents

[1]Dr. Ajibola A. Bayode https://orcid.org/0000-0003-2461-6208 (bayodea@run.edu.ng), Dr. Martins O. Omorogie https://orcid.org/0000-0001-9697-2960 (omorogiem@run.edu.ng)
Department of Chemical Sciences, Faculty of Natural Sciences, Redeemer's University, P.M.B. 230, 232101, Ede, Nigeria.

[2]Dr. Hamza Badamasi
Department of Chemistry, Federal University Dutse, Dutse, Jigawa State, Nigeria.

[3]Dr. Johnson Adedeji Olusola
Department of Geography and Planning Science, Ekiti State University, Ado Ekiti, Ekiti State, Nigeria.

[4]Dr. Johnson Adedeji Olusola
Institute of Ecology and Environmental Studies, Obafemi Awolowo University, Ile-Ife, 220005, Nigeria.

[5]Dr. Solomon S. Durodola, Dr. Odunayo T. Ore
Department of Chemistry, Obafemi Awolowo University, Ile-Ife, 220005, Nigeria.

[6]Dr. Olaniran K. Akeremale
Department of Science and Technology Education, Bayero University, 3011, Kano, Nigeria.

[7]Prof. Dr. Brigitte Helmreich, Dr. Martins O. Omorogie
Chair of Urban Water Systems Engineering, School of Engineering and Design, Technical University of Munich, Am Coulombwall 3, 85748 Garching, Germany.

[8]Dr. Martins O. Omorogie
Environmental Science and Technology Research Unit, African Centre of Excellence for Water and Environmental Research (ACEWATER), Redeemer's University, P.M.B. 230, Ede, 232101, Nigeria.

have been developed and investigated for the sequestration of dissolved phosphate, including biomass, biochars [25], clay minerals [17, 26], and various hybrid synthesized adsorbents [17]. Amongst all, clay minerals have been explored for the removal of various pollutants, but they are limited by their low adsorption capacity [5].

Kaolinite, a 2:1 clay mineral with the chemical formula $Al_2O_3{\cdot}2SiO_2{\cdot}2H_2O$, consisting of metal oxides such as aluminium oxide, silicon dioxide, magnesium oxide, and calcium oxide, is abundant in the environment [17]. It has found various applications over the years and proved to be an efficient and indispensable material for various industrial processes because of its thermal stability, excellent bonding ability, and great insulating properties. However, it is limited as an adsorbent because of its small surface area, difficulties in separation after the process, and its low cation exchange capacity [27].

Eggshell is a waste material with about 7 million tonnes produced annually all over the world [28]. A small amount of this waste is used as fertilizer, household cleansers, and feed for human and animal supplements. Large quantities are disposed into landfills. Various low-cost eggshell adsorbents have been used for the removal of phosphate, including iron oxyhydroxide eggshell [29], calcined eggshell [30], aluminum-modified eggshell [27], etc. The major component of eggshells is $CaCO_3$ [27], and it has been established by various researchers that $CaCO_3$ possesses an excellent capacity for phosphate adsorption [31], making any material containing it a good adsorbent for phosphate removal in wastewater.

Metal ion-modified biochars are increasingly gaining attention for the removal of phosphate from water because they are cost-effective and environmentally benign [32]. Zinc oxide has been established to be environmentally benign, and it has found vast application in various fields as it has proven to be a good engineering material [22, 33].

For this study, a zinc-modified hybrid eggshell sample was employed. The kaolinite clay acts as support, and the pulverized eggshell serves as a source of Ca, which has great affinity for the removal of phosphate. Zinc chloride acts as the activating agent, which influences the surface area and porosity of the activated carbon produced [34]. This study aimed at the modification of a hybrid eggshell that is eco-friendly for the removal of phosphate from water. The modification with zinc ameliorated the problem of poor phosphate adsorption using just the eggshell. A number of different published research papers on the use of eggshells for phosphate capture is available in the literature [35–41]. The adsorption of phosphate by ZnO-activated eggshells, supported on clay (kaolinite), is here reported for the first time to demonstrate its potential for phosphate removal from contaminated water.

2 Materials and Method

2.1 Materials

Kaolinite clay was obtained from Redemption City, Mowe (6.8085° N, 3.4367° E), Ogun State, and the eggshell was collected from the Cafeteria Kitchen of Redeemer's University, Ede (7.678163° N, 4.460089° E), Osun State. Zinc chloride (≥ 98 %), sodium hydroxide (99 %), potassium dihydrogen phosphate (99.9 %), ammonium metavanadate (99 %), ammonium molybdate hexahydrate (99 %), sodium chloride (99 %), hydrogen peroxide, and hydrochloric acid were purchased from Sigma Aldrich, Germany.

2.1.1 Pretreatment of the Kaolinite Clay and Eggshell

The kaolinite clay was purified according to protocols reported by Bayode et al. [22] via several washing and filtration processes with a mesh sieve after treatment with hydrogen peroxide [17]. The collected eggshells were pretreated by washing them in distilled water, and the clean eggshells were then transferred into the vacuum oven to dry at 105 ± 1 °C for 10 h. The dried eggshells were pulverized and stored in an airtight container labeled 'ES'.

2.1.1.1 Synthesis of Zinc-Modified Eggshells (ZnES)

Kaolinite clay, pulverized eggshells, and zinc chloride were weighed out in the ratio 1:1:2 and mixed in a beaker with 10 mL of 0.1 M sodium hydroxide. The mixture was placed in the oven and dried for a period of 24 h for the proper impregnation of the different constituents. The impregnated mixture was transferred into a microwave reactor, purged with nitrogen gas for 5 min, and calcined for 15 min at 500 W in a microwave oven. The product was allowed to cool in a desiccator. Afterwards, it was washed several times with deionized water until a clear solution was observed and the pH of the solution became neutral (pH 7.0). The material was dried in the oven at 105 ± 1 °C for 7 h, cooled in the desiccator, packed in a sample bottle, and labeled as 'ZnES'.

2.2 Characterization of the Adsorbents

ES and ZnES were characterized by Fourier transform infrared (FTIR) spectrophotometry (Shimadzu FT-IR 8400S, from 400 to 4000 cm^{-1}), X-ray diffraction (XRD) (Siemens D-5000), measured at 0.02° s^{-1}, ranging from 3.0° to 70° 2θ, scanning electron microscopy (SEM) (Jeol JSM 6510 SEM equipped with an energy dispersive X-ray (EDX) spectrometer from Oxford (INCAx-act SN detector)), and transmission electron microscopy (TEM) (field emission gun, 200 kV). Nitrogen sorption was done on a Quantachrome NOVA1000e Brunauer-Emmett-Teller (BET) system. The point of zero charge (PZC) was determined by using the salt addition method [42].

2.3 Batch Adsorption Studies

The batch adsorption kinetic studies were carried out in triplicate by agitation of 50 mL of 50 mg L^{-1} phosphate solution containing 0.1 g ZnES for 120 min. From that, 0.5 mL clear adsorbent-free solution was withdrawn using a micropipette at different intervals (between 1 and 120 min). The residual dissolved phosphate concentration was determined using the vanado-molybdophosphoric acid method of the American Public Health Association (APHA), by adding 1 mL of the

color-developing reagent to 3.5 mL of the withdrawn sample. The absorbance of the sample was then determined with a Shimadzu UV-Vis spectrophotometer at a wavelength of 420 nm.

The adsorption capacity, q_e (mg g^{-1}) was estimated using Eq. (1).

$$q_e = (C_o - C_e) \cdot \frac{V}{W} \quad (1)$$

where C_o and C_e (mg L^{-1}) are the initial and final concentrations of phosphate, respectively, V is the volume of the solution (L), and W is the mass (g) of ZnES used.

The adsorption isotherms of phosphate in ZnES were calculated using batch experiments. For this, 0.1 g ZnES was mixed with phosphate solutions with different initial concentrations ranging from 1, 10, 20, 30, and 40 to 50 mg L^{-1} for 120 min. At 120 min, the sample was withdrawn after the experiment for analysis.

The effect of the ZnES dosage on the uptake of phosphate was optimized by varying the weight of the adsorbent from 0.1 to 1.0 g; the effect of the pH on the adsorption process was also evaluated by varying the pH from 3.0 to 9.0, using 1.0 g adsorbent dose and the same initial phosphate concentration of 50 mg L^{-1}. Furthermore, the effect of the ionic strength was assessed by varying the NaCl concentration in the solution from 0 to 0.1 M at pH 3.0 and an adsorbent dose of 1.0 g. During the experiment, the initial concentrations of dissolved phosphate were maintained at 50 mg L^{-1}.

Experimental kinetics and isotherm data were fitted into some nonlinear equilibrium models, namely, Langmuir, Freundlich, Langmuir-Freundlich, pseudo-first-order model (PFOM), pseudo-second-order model (PSOM), and the Brouers-Weron-Sotolongo (BWS) model. The experimental data were analyzed using the quasi-Newton least squares algorithm in the KyPlot software 2.0 model (Kyens Lab Inc., Tokyo, Japan).

$$q_e = K_F C_e^{1/n} \quad (2)$$

$$q_e = \frac{q_{max_L} K_L C_e}{1 + K_L C_e} \quad (3)$$

$$q_e = \frac{q_{m_{LF}} (K_{LF} C_e)^{n_{LF}}}{1 + (K_{LF} C_e)^{n_{LF}}} \quad (4)$$

$$q_t = q_e\left(1 - e^{-k_1 t}\right) \quad (5)$$

$$q_t = q_e\left(1 - \left(1 + (n'Bws - 1)\left(\frac{t}{t_{n'BWS,\alpha}}\right)^{\alpha}\right)\right)^{-1/n'-1} \quad (6)$$

$$q_t = q_e - q_{t,1} e^{-k_1 t} - q_{t,2} e^{-k_2 t} \quad (7)$$

where K_F, n, K_L, $q_{max\,L}$, q_t, k_1, k_2, n', α, and $t^{1/2}$ are the Freundlich constant ((mg g^{-1})(L mg^{-1})$^{1/n}$), an empirical constant that represents the adsorption affinity, the Langmuir adsorption constant (L mg^{-1}), q_e for a complete monolayer (mg g^{-1}), the amounts of solute ions adsorbed at time t (min) by ZnES (mg g^{-1}), the pseudo-first-order rate constant (min^{-1}), and the pseudo-second-order rate constant (g mg^{-1}min^{-1}), respectively. n', α, and $t^{1/2}$ are the reaction order, fractional time index and time taken to reach 50% adsorption respectively.

3 Results and Discussion

3.1 Characterization of the Materials

3.1.1 Point of Zero Charge (pH_{pzc})

The pH_{pzc} was assessed to understand the net surface charge of the adsorbents [43]. The surface of the adsorbent becomes positively charged if the pH of the solution is less than the pH_{pzc}, which results in the adsorption of excess hydroxyl ions; on the other hand, the surface of the adsorbent becomes negatively charged if the pH of the solution is higher than the pH_{pzc} of the adsorbent, leading to the desorption of hydroxyl ions. Supporting Information Fig. S1 shows that the pH_{pzc} of the pristine adsorbent ES is 8.29, and upon modification of the eggshell with kaolinite and zinc, it changed to 8.61. This confirmed that the modification of the eggshell with zinc and kaolinite changed the surface characteristics of the eggshell. The adsorption process of negatively charged phosphate ions is favored at a pH lesser than the pH_{pzc}. In this regard, the adsorption of phosphate by ES and ZnES should be optimum within the pH range of 2.0–5.0.

3.1.2 FTIR Spectrophotometry

FTIR spectrometry was used to investigate the functional moieties present in ZnES and kaolinite. The most intense and wide peak was observed at 3377 cm^{-1} in ES and 3456 cm^{-1} in ZnES, suggesting the OH stretching bond [44, 45]. The peak was very intense in ZnES, which suggests that more OH groups exist on the surface of the ZnES, resulting from the presence of kaolinite that was added as part of the components for the synthesis, as shown in Fig. 1a. The weak bands at 2511 cm^{-1} in ES and 2530 cm^{-1} in ZnES suggest the C=O bonds from carbonates, as one of the major components present in ES [27, 46], while the peaks at 1434 and 868 cm^{-1} in both ZnES and ES suggest the C–O stretching and bending of $CaCO_3$ [47, 48]. In the fingerprint region, the peak at 710 cm^{-1} in both ZnES and ES suggests in-plane bending vibration of the O–C–O bond [49]. A new peak was formed at 792 cm^{-1}, which indicates the Si–O–Si inter-tetrahedral bridging bonds in SiO_2 present in kaolinite [22, 50]. The peak at 464 cm^{-1} confirms the presence of ZnO [22, 33] in ZnES because of the $ZnCl_2$ used for preparation.

3.1.3 XRD Analysis

Kaolinite shows characteristic quartz peaks at 2θ = 26.7°, 39.5°, 45.7°, 50.0°, 54.9°, 63.9°, and 68.2°, as shown in Fig. 1B. The anorthic phase of kaolinite is shown by peaks at 12.5° and 40.4°, and the quartz peaks at 21.1° and 50.1° and the kaolinite peaks at 26.9°, 45.7°, and 55.0° were observed in both kaolinite and ZnES [22, 33].

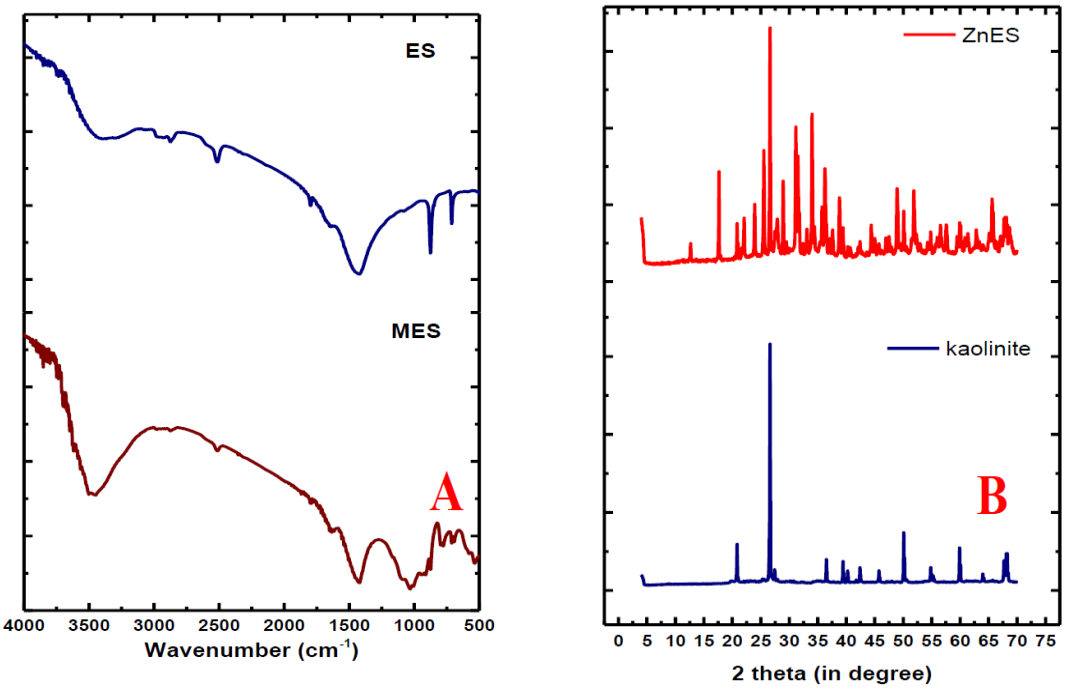

Figure 1. (A) FTIR spectra of the raw eggshells and ZnES, (B) XRD spectra of ZnES and kaolinite.

The absence of the kaolinite peaks at 12.5° and 25.0° was observed in the spectra of the ZnES, which may have been due to the change in the crystalline structure of the kaolinite clay during the modification process. The peaks at 36.6°, 39.3°, and 42.5° indicate the hexagonal wurtzite structure of Zn [33, 51]. Another ZnO phase, the zincite hexagonal phase, was also observed at 63.3°, 68.3° [50]. The ZnES spectra showed peaks at 39.0°, 47.3°, 57.7°, and 60.9°, indicating the hexagonal calcite phase, which was due to the eggshell present in the adsorbent. This result confirmed the successful synthesis of ZnES [27, 52].

3.1.4 SEM, EDX, and Electron Mapping Analysis

SEM was used to determine the surface availability of the ES and ZnES, as shown in Fig. 2A and 2B, respectively. The ES image showed that the surface was coarse, with flat particles of different sizes evenly distributed on the surface of the eggshell; a visible pore was also noticed on the surface in the image. The image of ZnES showed it to be smoother than the ES; the shapes and sizes of the adsorbent are rod-like, round, spherical, irregular, and sparsely distributed on the surface of the ZnES, and obvious pores were also noticed on the surface of the ZnES. These pores aid in the adsorption of phosphate onto the adsorbents.

The EDX spectra as shown in Fig. 2C and 2D further confirmed the results from the FTIR and XRD analyses. The ES comprises calcium, oxygen, and carbon as the major elements while magnesium is a minor constituent of the eggshell. From the literature, it has been reported that the eggshell is made up of $CaCO_3$ [49, 52]. The ZnES comprises calcium, oxygen, and carbon from the eggshell, zinc from the $ZnCl_2$ used to modify the adsorbent, and the aluminum, silicon, titanium, and iron stem from the kaolinite as a constituent of the adsorbent. The elements were evenly distributed on the surface of the ES and ZnES adsorbents, as shown in the electron mapping images (Supporting Information Figs. S2 and S3).

The TEM images reported in Fig. 2E and 2F showed that the microscopic structures of ES and ZnES possess a rough surface with spherical morphology, suggesting the random anchorage of both the oxides and carbonates of calcium and magnesium particles on the surface of the ES with a very good spread. The ZnES samples have different particle sizes, with the anchorage of zinc clustered together in a bunch on the surface and other elements like calcium and magnesium sparsely distributed on the surface of the ZnES.

3.1.5 BET Physisorptometry

The ES and ZnES both displayed a type-IV isotherm as classified by the International Union of Pure and Applied Chemistry (IUPAC) (Fig. 3A, B). This type of isotherm is typical of porous materials and it possesses an H3 adsorption-desorption loop typical of slit-shaped pores [42]. The BET surface areas of ES and ZnES were predicted as 0.188 and 7.33 m^2g^{-1}, respectively; the increase in the surface area of the modified eggshell (ZnES) could be the result of the modification of the eggshell with $ZnCl_2$. It has been reported by several researchers that modification with metal ions tends to change the surface characteristics; it either increases or decreases the surface area, pore volume, and pore diameter [43]. The pore volumes are 0.00298 and 0.0315 cm^3g^{-1} with pore sizes of 755.8 and 459.5 Å, respectively. The eggshell (ES) is microporous while the modified eggshell (ZnES) is mesoporous.

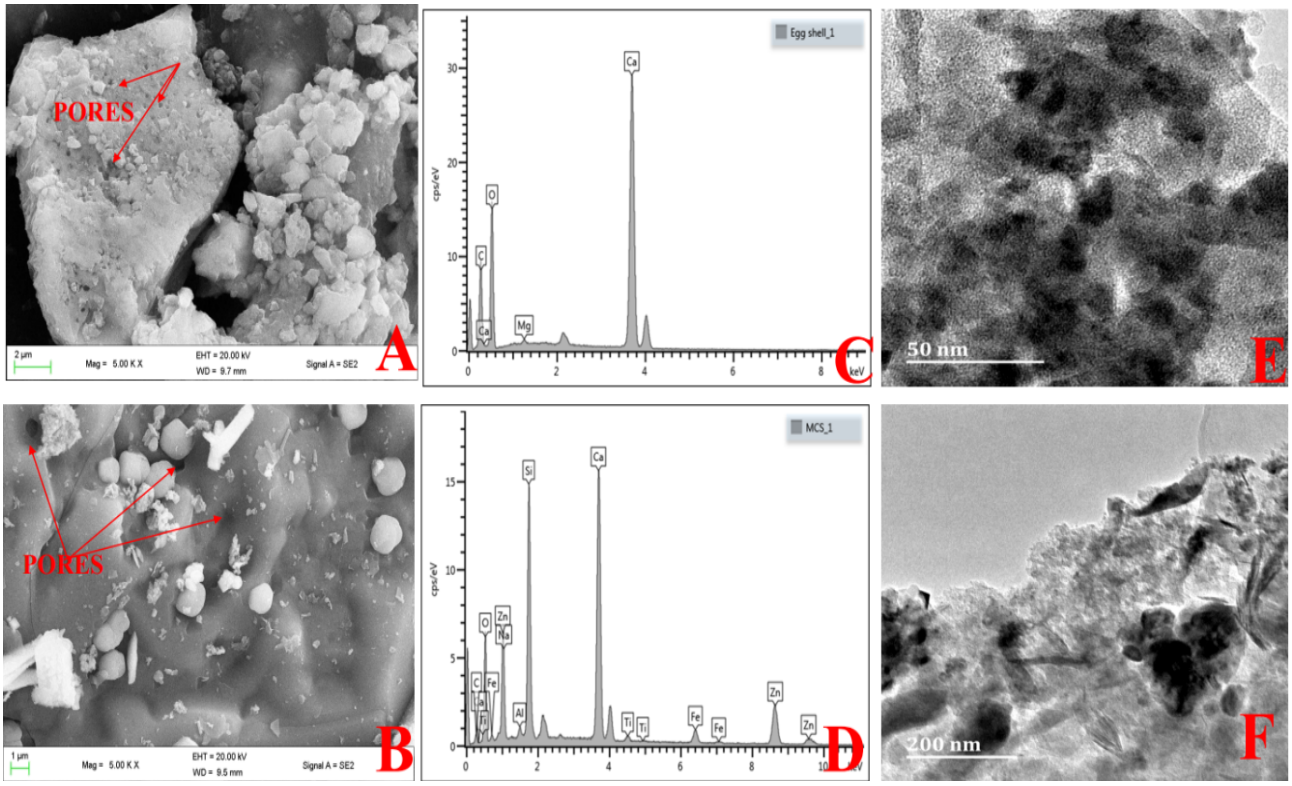

Figure 2. SEM images of (A) ES and (B) ZnES; EDX spectra of (C) ES and (D) ZnES; TEM images of (E) ES and (F) ZnES.

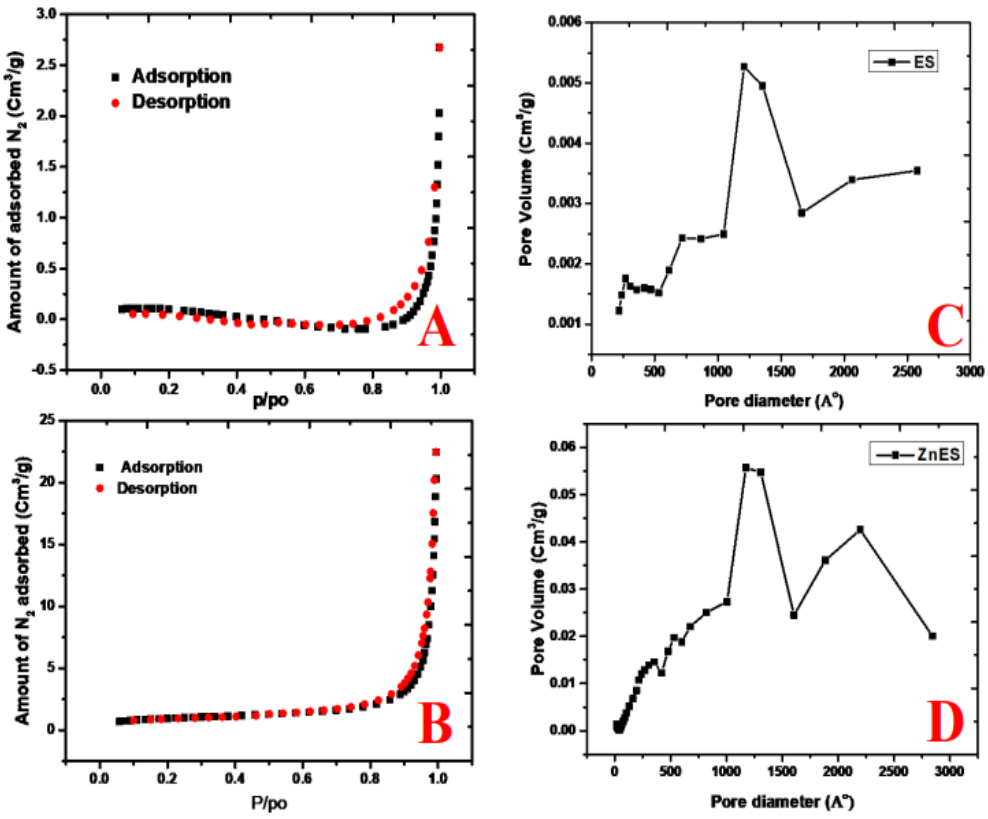

Figure 3. The BET nitrogen adsorption-desorption isotherms for (A) ES and (B) ZnES; pore size distribution for (C) ES and (D) ZnES.

3.2 Adsorption Studies

3.2.1 Preliminary Studies

To understand the influence/role of each component of the hybrid eggshell composite on/in the removal of dissolved phosphate from water, a series of experiments were carried out using the method described in Sect. 2.3, but the samples were withdrawn after 120 min. Fig. 4 shows that kaolinite alone and eggshell removed 12 % and 34 % of the phosphate in aqueous solutions, respectively. The modification of the eggshell with zinc chloride and kaolinite clay increased the surface area as confirmed by the BET result (Sect. 3.1.5) and also improved the surface functionalities and surface charge, which gives room for more adsorption sites for the removal of phosphate, resulting in an increased efficiency of 93 %. The kaolinite serves as a support and in the presence of zinc chloride, when it undergoes hydrolysis followed by calcination in the presence of the pulverized eggshell (ZnES), creates a macroporous material that is efficient for phosphate removal.

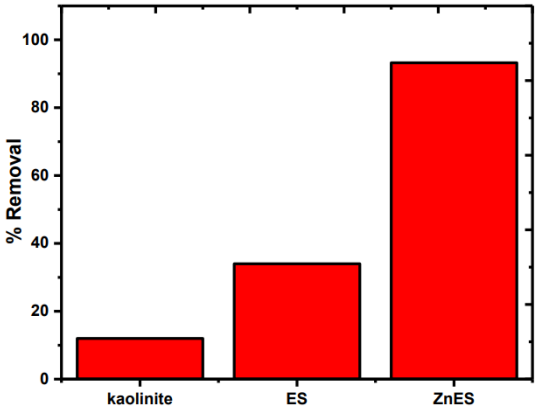

Figure 4. Efficiencies of the different components, kaolinite and eggshell, and the composite ZnES for the removal of phosphate in water.

3.2.2 Kinetic and Isotherm Studies

The experimental kinetics data obtained in this study were fitted into two- and three-parameter theoretical kinetic models, which are the PFOM, the PSOM, and the BWS model, to understand the adsorption process (Supporting Information Fig. S4A).

The kinetic parameter data of all the fitted models and the R^2 values determined by nonlinear regression analysis are reported in Tab. 1. To quantitatively compare the accuracy of the models in describing the experimental data obtained, the correlation coefficient was used.

Generally, based on the R^2 values obtained for the theoretical models fitted, the three-parameter model, BWS, provides the best fit with an R^2 value of 0.999. The BWS kinetic model parameter predicts a first-order rate of uptake of phosphate ions on ZnES, suggesting that the adsorption of phosphate onto ZnES works via multiple mechanisms of two or more physical and chemical processes, which include the chemical interaction of the phosphate solution and the ZnES by ligand exchange, hydrogen bonding, electrostatic interaction, outer-sphere complexation interaction, and weak van der Waals forces.

Table 1. Kinetic parameters for the removal of phosphate using the ZnES adsorbent.

Model	Parameter	Phosphate
PFOM	q_e [mg g^{-1}]	23.80
	K_{PF} [min^{-1}]	0.999
	R^2	0.942
PSOM	q_e [mg g^{-1}]	27.00
	K_{PS} [min^{-1}]	0.006
	R^2	0.978
BWS	q_e [mg g^{-1}]	25.01
	α	2.4×10^{-5}
	K_{BWS}	0.006
	R^2	0.999

The adsorption isotherm was used to estimate the quantity of phosphate adsorbed onto ZnES at equilibrium. The experimental data generated was fitted into three-parameter isotherm models, namely, the Langmuir, Freundlich, and Langmuir-Freundlich isotherm models (Supporting Information Fig. S4B).

The Langmuir-Freundlich isotherm model, a three-parameter isotherm, best fits the experimental data for the adsorption of phosphate using ZnES, followed by the Sips model (Langmuir-Freundlich > Sips > Langmuir > Freundlich), using the R^2 values as shown in Tab. 2.

The best-fitting model, Langmuir-Freundlich, is a combination of both the Langmuir and the Freundlich isotherm model used for predicting adsorption in heterogeneous systems, and it also overcomes the limiting factor associated with the Freund-

Table 2. Kinetic parameters for the removal of phosphate using the ZnES adsorbent.

Model	Parameter	Phosphate
Langmuir	q_m [mg g^{-1}]	51.977
	K_L [min^{-1}]	0.027
	R^2	0.991
Freundlich	K_F [mg g^{-1}]	2.897
	N	1.664
Langmuir-Freundlich	R^2	0.998
	q_e [mg g^{-1}]	30.775
	K_{LF}	0.0636
	N	2.156
	R^2	0.999

lich isotherm model (rise in the adsorbate concentration) [53]. When the concentration of the adsorbate is low, it functions as the Freundlich isotherm, but when the concentration is high, it functions as the Langmuir isotherm model, predicting its monolayer adsorption capacity characteristics [5]. The model predicts a maximum adsorption capacity of 30.8 mg g^{-1}, although the observed experimental adsorption capacity is 25.7 mg g^{-1}. The n_{LF} value is also lower than 1, which indicates that the Langmuir-Freundlich isotherm is favorable. The Freundlich isotherm fitting showed an n value greater than 1, which suggests that the adsorption was not appropriate.

3.2.3 Effect of the Adsorbent Dosage

It is vital to explore the effect of the adsorbent amount on the removal efficiency and to avoid the use of excess adsorbent leading to waste. It also affects the amount of adsorbed adsorbate; a different weight of ZnES adsorbent of 0.1–1.0 g was used for adsorption (50 mg L^{-1}). Fig. 5A shows that, as the weight of ZnES increases, the adsorption capacity towards phosphate decreases; this is because the amount of adsorption capacity is inversely proportional to the adsorbent weight.

The result showed an increase in the removal efficiency of phosphate as the adsorbent weight was increased. This may be because of an increase in the number of available active sites to enhance the adsorption activity.

3.2.4 Effect of the pH

The pH value is one of the most important factors controlling the adsorption of contaminants from water onto adsorbents because it can affect the surface charge of the pollutant [54]. The adsorption of phosphate by ZnES was studied at different pH values of 3.0–9.0, with an initial concentration of 50 mg L^{-1} and an adsorbent dose of 0.1 g in 50 mL phosphate solution over a time frame of 120 min.

The adsorption capacity and removal efficiency solely depend on the surface charge of the ZnES and the form in which the phosphate exists; at an acidic pH of 2.0, a neutral pH of 7.0, and an alkaline pH of 12.0, the dissociation equilibrium of phosphate is different, as shown in Eqs. (8)–(10) [31, 55].

$$H_2PO_4^- + H_2O \leftrightarrow H_3PO_4 + OH^- \quad (8)$$

$$HPO_4^{2-} + H_2O \leftrightarrow H_2PO_4^- + OH^- \quad (9)$$

$$PO_4^{3-} + H_2O \leftrightarrow HPO_4^{2-} + OH^- \quad (10)$$

The pH_{pzc} of ZnES as reported in Fig. 5B is 8.61. When the pH is less than the pH_{pzc}, the surface of the ZnES becomes positively charged and it becomes protonated, attracting $H_2PO_4^-$ and HPO_4^{2-}, which are negatively charged, to the surface of the ZnES. When the pH was higher than the pH_{pzc} of the ZnES, the surface became deprotonated, leading to a repulsive effect between ZnES and phosphate [56]. The maximum adsorption capacity and removal rate were observed at pH 3.0. A sharp decline was observed in both the adsorption capacity and removal rate from pH 7.0 to 9.0 because the hydroxyl ion competes with the HPO_4^{2-} ion for active sites on the surface of the ZnES, resulting in the decrease. It can be suggested that electrostatic interaction contributed to the adsorption of phosphate.

3.2.5 Effect of the Ionic Strength

The removal efficiency of phosphate with ZnES decreased drastically as the concentration of NaCl increased from 0 to 0.1 M, as presented in Fig. 6A. This is because the Cl^- ions compete with the phosphate ions for the available active sites on the ZnES adsorbent, leading to a decrease in adsorption capacity.

Also, the electrolyte can form outer-sphere complexes through electrostatic forces. The ionic strength strongly affects anions that are adsorbed through the outer sphere, which will lead to the competitive behavior between the phosphate and the electrolyte, impairing the adsorption performance [31, 55].

On the other hand, anions that are adsorbed by the inner sphere show either high adsorption in the presence of high ionic strength or the adsorption is slightly affected, suggesting that, if the adsorption of phosphate on ZnES occurred through the outer-sphere surface complex, then the adsorption will decrease with an increase in the ionic strength, which is the case in our study.

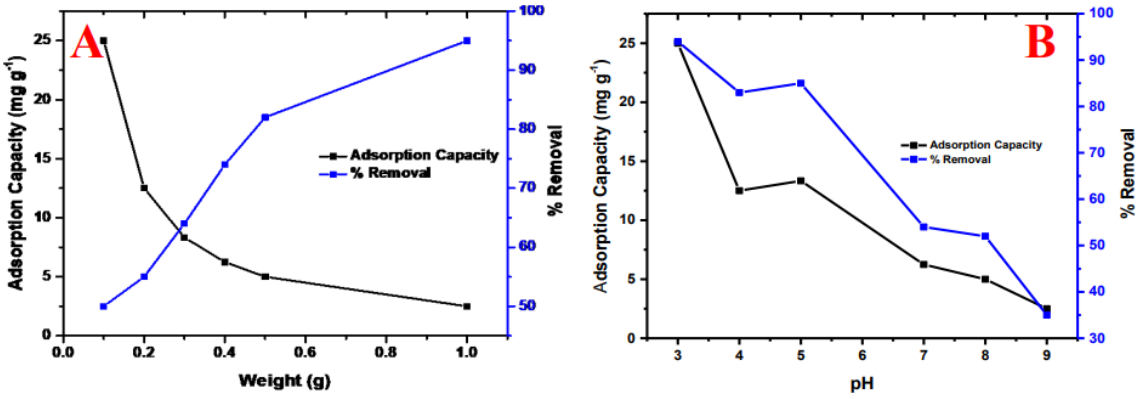

Figure 5. Effects of (A) the adsorbent dose and (B) the pH on the removal of phosphate using ZnES.

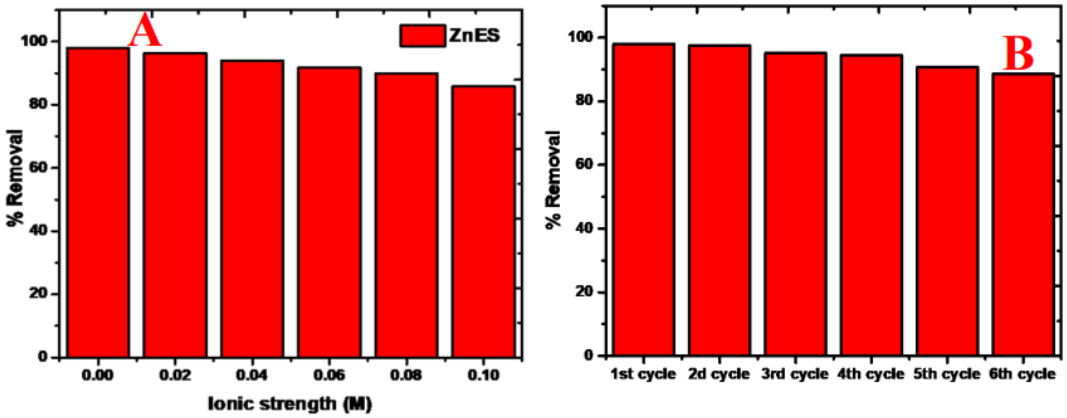

Figure 6. (A) Effect of the ionic strength on the removal of phosphate using ZnES and (B) reuse efficiency of ZnES over 6 cycles for the removal of phosphate.

3.3 Reusability Study

The regeneration of the adsorbent ZnES is highly desirable, as this will curb the indiscriminate disposal of the spent adsorbent into the environment. Also, testing the reusability capacity of the adsorbent is important in order to know how sustainable the adsorbent is [54]. The reusability experiment on the ZnES adsorbent was carried out using a cheap solvent (0.01 M NaOH), and the result obtained for the reusability is presented in Fig. 6B. It shows that there was no significant loss of efficiency over the four cycles with over ~90 % phosphate removal, but from the fifth cycle onwards, the efficiency decreased slightly to 82 %. This is still efficient, suggesting that ZnES is a potential benign adsorbent for the removal of phosphate in water.

3.4 Mechanism of Phosphate Adsorption by ZnES

The chemical and physical interactions between phosphate ions and the adsorbent ZnES govern their removal. Understanding the mechanism of adsorption is important because it takes into consideration all the results obtained from the experiments and gives insights into the major interaction playing the main role.

The adsorption of phosphate ions onto ZnES is controlled by electrostatic interaction; ZnES possesses a negative surface charge in water and the phosphate ion dissociates at different pH values, as stated in Sect. 3.2.4, Eqs. (8)–(10). Electrostatic interactions are highly dependent on the PZC of the adsorbent and the pH of the solution; it is favorable when the pH of the solution is lower than the pH_{pzc}, leading to the negatively charged phosphate ions being adsorbed electrostatically by positively charged ZnES particles, which was the case in our study.

$$Zn - OH + H_2PO_4 \rightarrow Zn - H_2PO_4 + OH^- \quad (11)$$

Apart from electrostatic interactions, there are precipitation, outer-sphere complexation interactions, and ion exchange interactions, in which the phosphate ion replaces other ions like Zn and Ca on the surface of the ZnES, as seen in Fig. 7.

The main component of eggshell is $CaCO_3$, the Ca present in ZnES existing as calcite. According to reports from various studies, it has been reported that the presence of Ca^{2+} enhanced the adsorption capacity of the adsorbent, with the combination of Ca^{2+} and PO_4^{3-} forming $Ca_5(PO_4)_3(OH)$, i.e. hydroxyapatite (precipitation reaction).

$$3PO_4^{3-} + 5Ca^{2+} + OH^- \rightarrow Ca_5(PO_4)_3OH \quad (12)$$

$$3HPO_4^{2-} + 5Ca^{2+} + 4OH^- \rightarrow Ca_5(PO_4)_3OH + 3H_2O \quad (13)$$

$$3H_2PO_4^- + 5Ca^{2+} + 7OH^- \rightarrow Ca_5(PO_4)_3OH + 6H_2O \quad (14)$$

In the ion exchange mechanism, the phosphate ion replaces an ion from the structure of the ZnES biochar. There are two possible means of complex formation during the adsorption

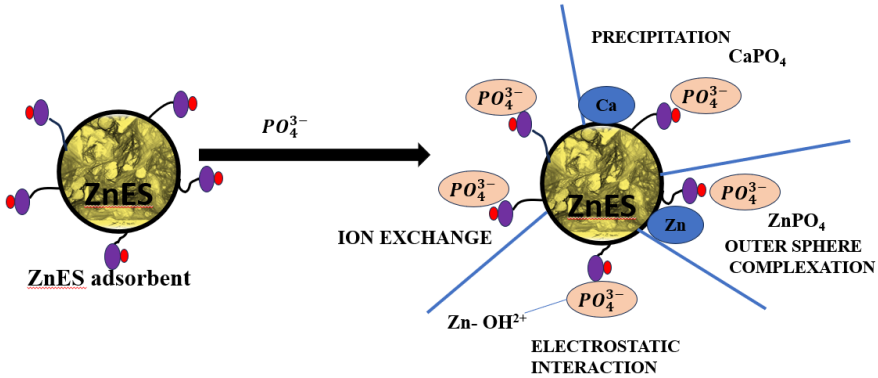

Figure 7. Adsorption mechanism of the removal of phosphate ions by modified eggshell (ZnES).

process, which are the inner-sphere and the outer-sphere complexation. In the outer-sphere complexation, a weak bond, such as a hydrogen bond, occurs on the outer surface of the adsorbent, while for the inner-sphere complex, there is a chemical interaction between the adsorbent and the adsorbate. As the result from Sect. 3.2.5, the effect of the ionic strength was used to determine the inner- or outer-sphere complexation. Fig. 6A confirms that an outer-sphere complex is formed during the adsorption process, as there was significant reduction in the adsorption capacity as the ionic strength of NaCl increased [57]. The transition metal in the component of the zinc material in the form of zinc oxide has empty d-orbitals, which can receive electrons from the negatively charged phosphate ions, which in turn increases the adsorption of the phosphate from the phosphate solution [58].

3.5 Simple Economics/Cost Evaluation of ZnES

A comparison of the adsorption capacities of various adsorbents for phosphate ions is provided in Tab. 3. The value of q_{max} in this study (25.1 mg g^{-1}) is larger than some of those in the previous report. This suggested that phosphate ions could be readily adsorbed on ZnES.

Table 3. Comparison of the adsorption capacities of adsorbents for the removal of phosphate.

Adsorbent	Adsorption capacity [mg g^{-1}]	Reference
Iron-hydroxide eggshell	14.5	[35]
Zr-loaded fibrous adsorbent	1.73	[63]
Fe_3O_4 nanoparticles	5.03	[64]
Fe_2O_3	7.49	[65]
Fe/$CaCO_3$_PVA 1:1	16.7	[65]
Fe/$CaCO_3$_PVA 1:5	1.91	[65]
Fe/$CaCl_2$_No PVA	17.0	[65]
Fe/$MgCO_3$_PVA 1:1	16.1	[65]
Zr-loaded graphite oxide	18.7	[66]
One-step method Fe_3O_4@ZrO_2	24.9	[67]
Zirconium ferrite	13.0	[68]
Aluminum chloride-eggshell	19.1	[27]
Three-step method zirconium ferrite	16.5	[68]
ZnES	25.1	This study

One of the major aims of this study was to synthesize a low-cost adsorbent that would be used for the total capture of phosphate from water matrices. To ascertain that our as-prepared adsorbent ZnES is cost-effective and sustainable, the cost must be estimated and calculated. The total cost takes into consideration the different steps involved in the synthesis, such as raw material sourcing, washing, drying, calcination, and chemical modification/activation, and the reuse potential [59–62]. The total cost synthesis of ZnES is presented in Supporting Information Tab. S1.

The total cost for the synthesis of 1 kg of ZnES is USD 4.17. When compared with other adsorbents in use, such as graphene oxide, multi-walled carbon nanotubes, and graphitic carbon nitride, it was found to be far cheaper, which makes it sustainable.

Furthermore, the adsorption cost was calculated using the formula

$$\text{Adsorption cost} = \frac{\text{USD}}{\text{g of Adsorbate}} = \frac{\left(\text{Chemical purchase}\left[\frac{\text{USD}}{\text{g}}\right] + \text{Energy cost}\left[\frac{\text{USD}}{\text{g}}\right]\text{kWh}\right)}{\text{Adsorption capacity}\left[\frac{\text{mg}}{\text{g}}\right] \times [10^{-3}]} \quad (15)$$

The estimation of the adsorbent cost for the removal of phosphate in water was calculated to be USD 2.48 per gram adsorbate, which is quite affordable and can be used as point of the point-of-use system purposes or can be scaled up for industrial applications.

The main material of ZnES, eggshell, is an abundant waste all over the world that is dumped in landfills; another constituent, kaolinite, is also abundant in the environment because it is a naturally occurring mineral. Therefore, the total cost of ZnES is low as compared to other conventional adsorbents and industrial by-products. The ZnES can also be regenerated and used over and over, which is sustainable.

4 Conclusion

Zn-modified eggshells have a higher adsorption capacity for dissolved phosphate from water compared to unmodified pulverized eggshells. The obtained pH_{pzc} of ZnES favored the adsorption of phosphate at a pH less than the pH_{pzc} value. Maximum adsorption was obtained at pH 3.0. Moreover, the phosphate removal efficiency achieved in the experiments was high (93.3 %), and a maximum capacity of 25.1 mg g^{-1} of phosphate was observed. Sorption study experimental data suggest the first-order uptake of phosphate onto ZnES, which could be by multiple mechanisms of two or more physical and chemical processes, such as ligand exchange, hydrogen bonding, electrostatic interaction, and weak van der Waals forces. The removal efficiency of phosphate with ZnES is reduced greatly with the presence of more electronegative anions like Cl^-, because of the competition for active sites on the adsorbent, which suggests the adsorption of phosphate was through outer-sphere surface complexation. The economic advantage of the adsorbent was achieved from the reusability study, which indicated no significant loss of its efficiency over four cycles with ~90 % phosphate removal, suggesting ZnES to be a potential adsorbent for the removal of phosphate in water. The cost analysis of the prepared adsorbent was carried out and further confirmed ZnES to be cheap and sustainable.

Supporting Information

Supporting Information for this article can be found under DOI: https://doi.org/10.1002/ceat.202300176.

The authors have declared no conflict of interest.

Acknowledgments

Dr. Ajibola A. Bayode is grateful for the support received from the Institute of Chemistry, University of Sao Paulo, Sao Carlos, Brazil, and University of Kwazulu Natal, Westville Campus, Durban, South Africa, in characterizing the synthesized adsorbents. Dr. Martins O. Omorogie (NGA-1201082-HFST-E) and Prof. Dr. Brigitte Helmreich greatly acknowledge the technical support of the Alexander von Humboldt Foundation, Carl Friedrich von Siemens Foundation, Chair of Urban Water Systems Engineering, Technical University of Munich, Garching, Germany, and the Department of Chemical Sciences, Faculty of Natural Sciences, Redeemer's University, Ede, Nigeria. Open access funding enabled and organized by Projekt DEAL.

Symbols used

C_e	[mg g^{-1}]	equilibrium concetration
C_o	[mg g^{-1}]	initial concentration
E	[%]	removal efficiency
K_{BWS}	[min^{-1}]	Brouers-Weron-Sotolongo adsorption capacity
K_F	[(mg g^{-1})(mg L^{-1}) $^{-1/\eta F}$]	Freundlich constant
K_L	[L mg^{-1}]	Langmuir constant
K_{LF}	[L mg^{-1}]	Langmuir-Freundlich constant
K_{PF}	[min^{-1}]	pseudo-first-order rate constant
K_{PS}	[min^{-1}]	pseudo-second-order rate constant
n	[–]	number of experiments
η_F	[–]	Freundlich heterogenicity constant
q	[mg g^{-1}]	adsorption capacity
q_1	[mg g^{-1}]	pseudo-first-order adsorption capacity
q_2	[mg g^{-1}]	pseudo-second-order adsorption capacity
q_e	[mg g^{-1}]	equilibrium adsorption capacity
q_i, exp	[mg g^{-1}]	experimental adsorption capacity
q_i, model	[mg g^{-1}]	predicted value of the adsorption capacity
q_t	[mg g^{-1}]	adsorption capacity as a function of the time
R^2	[–]	correlation frequency
S_{BET}	[m^{2}g^{-1}]	BET surface area
t	[min]	time
V	[L]	contaminant volume
W	[g]	adsorbent mass

Greek symbol

λ_{max}	[nm]	wavelength of maximum absorption

Abbreviations

BET	Brunauer-Emmett-Teller
BWS	Brouers-Weron-Sotolongo
EDX	energy-dispersive X-ray
ES	eggshells
FTIR	Fourier transform infrared
PFOM	pseudo-first-order model
PSOM	pseudo-second-order model
PZC	point of zero charge
SEM	scanning electron microscopy
TEM	transmission electron microscopy
XRD	X-ray diffraction
ZnES	zinc-modified eggshells

References

[1] C. P. Mainstone, W. Parr, *Sci. Total Environ.* **2002**, *282*, 25–47.
[2] C. Trépanier, S. Parent, Y. Comeau, J. Bouvrette, *Water Res.* **2002**, *36 (4)*, 1007–1017.
[3] D. A. Lemley, J. B. Adams, G. M. Rishworth, C. Bouland, *Sci. Tot. Environ.* **2019**, *693*, 133601.
[4] European Water Framework Directive (2000/60/EC), *Off. J.Eur. Communities: Legis.* **2000**, *327*, 1–73.
[5] E. I. Unuabonah, F. O. Agunbiade, M. O. Alfred, T. A. Adewumi, C. P. Okoli, M. O. Omorogie, M. O. Akanbi, A. E. Ofomaja, A. Taubert, *J. Cleaner Prod.* **2017**, *164*, 652–663.
[6] M. Oliveira, A. V. Machado, R. Nogueira, *Water, Air, Soil Pollut.* **2012**, *223 (8)*, 4831–4840. DOI: https://doi.org/10.1007/s11270-012-1239-9
[7] S. Yang, Y. Zhao, R. Chen, C. Feng, Z. Zhang, Z. Lei, Y. Yang, *J. Colloid Interface Sci.* **2013**, *396*, 197–204.
[8] L. Deng, Z. Shi, *J. Alloys Compd.* **2015**, *637*, 188–196.
[9] Y. Ye, H. H. Ngo, W. Guo, Y. Liu, J. Li, Y. Liu, X. Zhang, H. Jia, *Sci. Total Environ.* **2017**, *576*, 159–171. DOI: https://doi.org/10.1016/j.scitotenv.2016.10.078
[10] Y. Yang, X. Shi, W. Ballent, B. K. Mayer, *Water Environ. Res.* **2017**, *89 (12)*, 2122–2135. DOI: https://doi.org/10.2175/106143017X15054988926424
[11] L. Kong, Y. Tian, N. Li, Y. Liu, J. Zhang, J. Zhang, W. Zuo, *Appl. Clay Sci.* **2018**, *162*, 507–517. DOI: https://doi.org/10.1016/j.clay.2018.07.005
[12] Y.-K. Geng, Y. Wang, X.-R. Pan, G.-P. Sheng, *Bioresour. Technol.* **2018**, *247*, 471–476. DOI: https://doi.org/10.1016/j.biortech.2017.09.118
[13] T. E. Bektaş, B. K. Uğurluoğlu, B. Tan, *Water Pract. Technol.* **2021**, *16 (4)*, 1343–1354. DOI: https://doi.org/10.2166/wpt.2021.072
[14] Y. He, H. Lin, Y. Dong, L. Wang, *Appl. Surf. Sci.* **2017**, *426*, 995–1004. DOI: https://doi.org/10.1016/j.apsusc.2017.07.272

[15] O. T. Ore, A. O. Adeola, A. A. Bayode, D. T. Adedipe, P. N. Nomngongo, *Environ. Chem. Ecotoxicol.* **2023**, *5*, 9–23. DOI: https://doi.org/10.1016/j.enceco.2022.10.004

[16] M. O. Omorogie, M. T. Agbadaola, A. M. Olatunde, B. Helmreich, J. O. Babalola, *Green Chem. Lett. Rev.* **2022**, *15 (1)*, 51–60.

[17] M. O. Omorogie, F. O. Agunbiade, M. O. Alfred, O. T. Olaniyi, T. A. Adewumi, A. A. Bayode, A. E. Ofomaja, E. B. Naidoo, C. P. Okoli, T. A. Adebayo, *Chem. Pap.* **2018**, *72 (2)*, 409–417.

[18] M. O. Omorogie, F. O. Ilesanmi, M. O. Alfred, B. Helmreich, *New J. Chem.* **2022**, *46 (43)*, 20918–20931.

[19] M. Huber, K. Athanasiadis, B. Helmreich, *Environ. Challenges* **2020**, *1*, 100008.

[20] A. A. Bayode, M. T. Folorunso, B. Helmreich, M. O. Omorogie, *ACS Omega* **2023**, *8 (8)*, 7956–7967.

[21] M. O. Omorogie, J. O. Babalola, E. I. Unuabonah, J. R. Gong, *Clean Technol. Environ. Policy* **2016**, *18*, 171–184.

[22] A. A. Bayode, F. O. Agunbiade, M. O. Omorogie, R. Moodley, O. Bodede, E. I. Unuabonah, *Environ. Sci. Poll. Res.* **2020**, *27 (9)*, 9957–9969.

[23] A. O. Adeola, B. A. Abiodun, D. O. Adenuga, P. N. Nomngongo, *J. Contam. Hydrol.* **2022**, *248*, 104019. DOI: https://doi.org/10.1016/j.jconhyd.2022.104019

[24] W. Huang, Y. Zhang, D. Li, *J. Environ. Manage.* **2017**, *193*, 470–482.

[25] D. Chen, X. Xiao, K. Yang, *RSC Adv.* **2016**, *6 (42)*, 35332–35339. DOI: https://doi.org/10.1039/C6RA05034D

[26] M. W. Kamiyango, W. R. L. Masamba, S. M. I. Sajidu, E. Fabiano, *Phys. Chem. Earth, Parts A/B/C* **2009**, *34 (13)*, 850–856. DOI: https://doi.org/10.1016/j.pce.2009.07.012

[27] Z. Guo, J. Li, Z. Guo, Q. Guo, B. Zhu, *Environ. Sci. Pollut. Res. Int.* **2017**, *24 (16)*, 14525–14536.

[28] B. Ngayakamo, A. P. Onwualu, *Heliyon* **2022**, *8 (6)*, e09649.

[29] P. V. Almeida, A. F. Santos, D. V. Lopes, L. M. Gando-Ferreira, M. J. Quina, *J. Water Process Eng.* **2020**, *36*, 101248. DOI: https://doi.org/10.1016/j.jwpe.2020.101248

[30] A. F. Santos, A. L. Arim, D. V. Lopes, L. M. Gando-Ferreira, M. J. Quina, *J. Environ. Manage.* **2019**, *238*, 451–459. DOI: https://doi.org/10.1016/j.jenvman.2019.03.015

[31] N. Oladoja, R. Adelagun, A. Ahmad, I. Ololade, *Process Saf. Environ. Prot.* **2015**, *98*, 296–308.

[32] Y. Feng, Y. Luo, Q. He, D. Zhao, K. Zhang, S. Shen, F. Wang, *J. Environ. Chem. Eng.* **2021**, *9 (3)*, 105267.

[33] A. A. Bayode, E. M. Vieira, R. Moodley, S. Akpotu, A. S. S. de Camargo, D. Fatta-Kassinos, E. I. Unuabonah, *Chem. Eng. J.* **2021**, *420*, 127668. DOI: https://doi.org/10.1016/j.cej.2020.127668

[34] Arneli, Z. F. Safitri, A. W. Pangestika, F. Fauziah, V. N. Wahyuningrum, Y. Astuti, *IOP Conf. Ser.: Mater. Sci. Eng.* **2017**, *172*, 012007.

[35] N. Y. Mezenner, A. Bensmaili, *Chem. Eng. J.* **2009**, *147 (2/3)*, 87–96.

[36] T. E. Köse, B. Kıvanç, *Chem. Eng. J.* **2011**, *178*, 34–39.

[37] Q. He, Y. Luo, Y. Feng, K. Xie, K. Zhang, S. Shen, Y. Luo, F. Wang, *Mater. Res. Express.* **2020**, *7 (11)*, 115603.

[38] Y. Zhang, H. Li, Y. Zhang, F. Song, X. Cao, X. Lyu, Y. Zhang, J. Crittenden, *Adsorpt. Sci. Technol.* **2018**, *36 (3/4)*, 999–1017.

[39] X. Liu, F. Shen, X. Qi, *Sci. Total Environ.* **2019**, *666*, 694–702.

[40] L. Wang, J. Wang, Y. Wei, *Colloids Surf., A* **2021**, *622*, 126589.

[41] H. Cao, X. Wu, S. S. A. Syed-Hassan, S. Zhang, S. H. Mood, Y. J. Milan, M. Garcia-Perez, *Bioresour. Technol.* **2020**, *318*, 124063.

[42] A. A. Bayode, D. M. dos Santos, M. O. Omorogie, O. D. Olukanni, R. Moodley, O. Bodede, F. O. Agunbiade, A. Taubert, A. S. S. de Camargo, H. Eckert, E. M. Vieira, E. I. Unuabonah, *J. Water Process Eng.* **2021**, *40*, 101865. DOI: https://doi.org/10.1016/j.jwpe.2020.101865

[43] O. A. Olalekan, A. J. Campbell, A. Adewuyi, W. J. Lau, O. G. Adeyemi, *Results Chem.* **2022**, *4*, 100457.

[44] M. Baláž, J. Ficeriová, J. Briančin, *Chemosphere* **2016**, *146*, 458–471. DOI: https://doi.org/10.1016/j.chemosphere.2015.12.002

[45] M. Tamang, K. K. Paul, *J. Indian Chem. Soc.* **2022**, *99 (1)*, 100251. DOI: https://doi.org/10.1016/j.jics.2021.100251

[46] J. Yang, M. Zhang, H. Wang, J. Xue, Q. Lv, G. Pang, *J. Environ. Manage.* **2021**, *9 (5)*, 105354. DOI: https://doi.org/10.1016/j.jece.2021.105354

[47] J. Boro, L. J. Konwar, D. Deka, *Fuel Process. Technol.* **2014**, *122*, 72–78. DOI: https://doi.org/10.1016/j.fuproc.2014.01.022

[48] I. B. Laskar, K. Rajkumari, R. Gupta, S. Chatterjee, B. Paul, S. L. Rokhum, *RSC Adv.* **2018**, *8 (36)*, 20131–20142. DOI: https://doi.org/10.1039/C8RA02397B

[49] A. Rahmani-Sani, P. Singh, P. Raizada, E. C. Lima, I. Anastopoulos, D. A. Giannakoudakis, S. Sivamani, T. A. Dontsova, A. Hosseini-Bandegharaei, *Bioresour. Technol.* **2020**, *297*, 122452. DOI: https://doi.org/10.1016/j.biortech.2019.122452

[50] S. Mustapha, J. O. Tijani, M. M. Ndamitso, S. A. Abdulkareem, D. T. Shuaib, A. K. Mohammed, A. Sumaila, *Sci. Rep.* **2020**, *10 (1)*, 13068. DOI: https://doi.org/10.1038/s41598-020-69808-z

[51] B. W. Shivaraj, H. N. N. Murthy, M. Krishna, B. S. Satyanarayana, *Procedia Mater. Sci.* **2015**, *10*, 292–300. DOI: https://doi.org/10.1016/j.mspro.2015.06.053

[52] Y. M. Isa, C. Harripersadth, P. Musonge, A. Sayago, M. G. Morales, *South African J. Chem. Eng.* **2020**, *34 (1)*, 142–150. DOI: https://doi.org/10.1016/j.sajce.2020.08.002

[53] K. Y. Foo, B. H. Hameed, *Chem. Eng. J.* **2010**, *156 (1)*, 2–10. DOI: https://doi.org/10.1016/j.cej.2009.09.013

[54] A. Adewuyi, R. A. Oderinde, *Curr. Res. Green Sustainable Chem.* **2022**, *5*, 100320. DOI: https://doi.org/10.1016/j.crgsc.2022.100320

[55] N. A. Oladoja, A. L. Ahmad, O. A. Adesina, R. O. A. Adelagun, *Chem. Eng. J.* **2012**, *209*, 170–179.

[56] W. Gu, Q. Xie, C. Qi, L. Zhao, D. Wu, *Powder Technol.* **2016**, *301*, 723–729.

[57] A. Nakarmi, S. E. Bourdo, L. Ruhl, S. Kanel, M. Nadagouda, P. K. Alla, I. Pavel, T. Viswanathan, *J. Environ. Manage.* **2020**, *272*, 111048.

[58] Q. Zheng, L. Yang, D. Song, S. Zhang, H. Wu, S. Li, X. Wang, *Chemosphere* **2020**, *259*, 127469.

[59] A. K. Sakhiya, P. Baghel, A. Anand, V. K. Vijay, P. Kaushal, *Bioresour. Technol. Rep.* **2021**, *15*, 100774. DOI: https://doi.org/10.1016/j.biteb.2021.100774

[60] S. Praveen, R. Gokulan, T. B. Pushpa, J. Jegan, *J. Indian Chem. Soc.* **2021**, *98 (8)*, 100107. DOI: https://doi.org/10.1016/j.jics.2021.100107

[61] S. O. Akpotu, P. N. Diagboya, I. A. Lawal, S. O. Sanni, A. Pholosi, M. G. Peleyeju, F. M. Mtunzi, A. E. Ofomaja, *Chem. Eng. J.* **2023**, *453*, 139771. DOI: https://doi.org/10.1016/j.cej.2022.139771
[62] J. O. Ighalo, F. O. Omoarukhe, V. E. Ojukwu, K. O. Iwuozor, C. A. Igwegbe, *Cleaner Chem. Eng.* **2022**, *3*, 100042. DOI: https://doi.org/10.1016/j.clce.2022.100042
[63] M. R. Awual, A. Jyo, T. Ihara, N. Seko, M. Tamada, K. T. Lim, *Water Res.* **2011**, *45 (15)*, 4592–4600. DOI: https://doi.org/10.1016/j.watres.2011.06.009
[64] S.-Y. Yoon, C.-G. Lee, J.-A. Park, J.-H. Kim, S.-B. Kim, S.-H. Lee, J.-W. Choi, *Chem. Eng. J.* **2014**, *236*, 341–347. DOI: https://doi.org/10.1016/j.cej.2013.09.053
[65] C. Han, J. Lalley, N. Iyanna, M. N. Nadagouda, *Mater. Chem. Phys.* **2017**, *198*, 115–124. DOI: https://doi.org/10.1016/j.matchemphys.2017.05.038
[66] E. Zong, D. Wei, H. Wan, S. Zheng, Z. Xu, D. Zhu, *Chem. Eng. J.* **2013**, *221*, 193–203. DOI: https://doi.org/10.1016/j.cej.2013.01.088
[67] Z. Wang, M. Xing, W. Fang, D. Wu, *Appl. Surf. Sci.* **2016**, *366*, 67–77. DOI: https://doi.org/10.1016/j.apsusc.2016.01.059
[68] B. K. Biswas, K. Inoue, K. N. Ghimire, H. Harada, K. Ohto, H. Kawakita, *Bioresour. Technol.* **2008**, *99 (18)*, 8685–8690. DOI: https://doi.org/10.1016/j.biortech.2008.04.015

